Biochemistry
Article
Cite This: Biochemistry XXXX, XXX, XXX−XXX
pubs.acs.org/biochemistry

A Novel Determinant of PSMD9 PDZ Binding Guides the Evolution of the First Generation of Super Binding Peptides

Mahalakshmi Harish,[†,‡] Srinivasaraghavan Kannan,[§] Srivalli Puttagunta,[†,#] Mohan R. Pradhan,[§] Chandra S. Verma,[*,§,∥,⊥] and Prasanna Venkatraman[*,†,‡,¶]

[†]Protein Interactome Lab for Structural and Functional Biology, Advanced Centre for Treatment, Research and Education in Cancer, Sector 22, Kharghar, Navi Mumbai, Maharashtra, India 410210

[‡]Homi Bhabha National Institute, 2nd floor, BARC Training School Complex, Anushaktinagar, Mumbai, Maharashtra, India 400094

[§]Bioinformatics Institute (BII), A*STAR, 30 Biopolis Street, 07-01 Matrix, Singapore 138671

[∥]Department of Biological Sciences, National University of Singapore, 16 Science Drive, Singapore 117558

[⊥]School of Biological Sciences, Nanyang Technological University, 60 Nanyang Drive, Singapore 637551

Supporting Information

ABSTRACT: The PDZ domain is one of the most widespread protein interaction domains found in nature. Due to their integral role in numerous biological functions, their ability to act as scaffolds for signal amplification, and the occurrence of mutations linked to human diseases, PDZ domains are attractive therapeutic targets. On the basis of the differential binding affinities of selected C-terminal peptides of the human proteome for one such PDZ domain (PSMD9) and by exploring structure−activity relationships, we design and convert a low-affinity tetrapeptide (∼439 μM) to a tight binding sequence (∼5 μM). The peptide inhibits PSMD9−hnRNPA1 interactions that are critical in basal and stimulus-induced NF-κB signaling and a potential therapeutic target in cancers, including chemotherapy or radiation-induced therapy resistance. Extensive application of computer modeling, including ligand mapping and all-atom molecular dynamics simulations, helps us to rationalize the structural basis for the huge differences in binding affinity and inform us about the residue-wise contributions to the binding energy. Our findings are in accord with the classical preference of the (PSMD9) PDZ domain for C-terminal sequences that contain hydrophobic residues at the P0 (C-terminal) position. In addition, for the first time, we identify a hitherto unknown occupancy for cysteine at the P−2 position that drives high-affinity interaction in a PDZ domain.

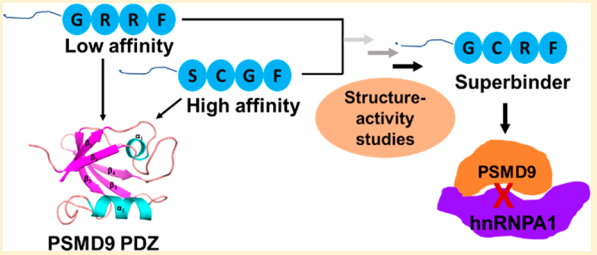

All cellular processes are driven by the complex interplay of protein−protein interactions (PPIs), carefully orchestrated to function in a spatiotemporal manner. These interactions are governed by protein interaction domains that bind to target proteins via specialized binding interfaces. The interfaces have evolved to ensure a high degree of specificity for a target protein and at the same time are malleable enough to recognize a variety of interacting partners. In the majority of domains involved in protein−protein interactions, the binding site is well-studied as it is often the target for designing small molecule or peptide-based inhibitors of the PPIs. Many inhibitors that block signaling cascades capitalize on these conserved regions or "hot spots" of binding sites. One such conserved well-studied protein interaction domain is the ubiquitous PDZ domain (PDZ is an acronym of PSD-95, Discs-large, ZO-I),[1] found in many synaptic junctions, where signaling molecules are concentrated. PDZ domains predominantly bind to the C-termini of interacting partner proteins, although some of them bind to internal sequences. Typically, this domain is characterized by a conserved fold comprising six β-sheets (β1−β6) capped by two α-helices (α1 and α2) (Figure S2).[2,3] Because PDZ domains dictate the direction and amplitude of signaling cascades by acting as scaffolds recruiting other proteins, mutations in this domain are associated with diseases such as cancer and neurodegenerative disorders.[4,5] All of the properties mentioned above make PDZ domains attractive therapeutic targets.[6] However, the development of inhibitors for targeting PDZ domain−peptide interactions with specificity is a challenge because a single PDZ domain can recognize a wide variety of client proteins, and many of them have very similar binding interfaces.[6] This demands an in-depth investigation of the target binding interface at high resolution to understand the exquisite specificity.

Previously, using a C-terminal peptide library representing the human proteome, we identified several novel interacting partners of PSMD9.[7] Two of these proteins were of special interest: hnRNPA1 (carrying the GRRF motif at the C-terminus) and growth hormone (carrying the SCGF motif at

Received: April 8, 2019
Revised: July 9, 2019
Published: July 9, 2019

Downloaded via NANYANG TECHNOLOGICAL UNIV on August 6, 2019 at 02:42:15 (UTC).
See https://pubs.acs.org/sharingguidelines for options on how to legitimately share published articles.

© XXXX American Chemical Society

DOI: 10.1021/acs.biochem.9b00308
Biochemistry XXXX, XXX, XXX−XXX

the C-terminus). The binding affinities of these two C-terminal peptides for PSMD9 were dramatically different (the K_D of GRRF was ~600 μM, and the K_D of SCGF was ~8 μM).

Natural variants of the GRRX series (also from the human proteome) carrying a hydrophobic residue (X = I, L, or C) at the P0 position retained binding to PSMD9. However, a mutant peptide, GRRG (G at the P0 position), neither bound to PSMD9 nor was able to inhibit the binding of hnRNPA1 to PSMD9. These results established that like other classical PDZ domains, the PDZ domain of PSMD9 preferred a hydrophobic residue at the P0 position. In sharp contrast, the mutant SCGG peptide was as good as the wild-type (WT) peptide SCGF in inhibiting the binding of GH to PSMD9.[7]

These observations yielded an interesting puzzle. Two peptides, each carrying the same bulky hydrophobic residue at the P0 position, which is the hallmark of peptide recognition by PDZ domain proteins, show a ~70-fold difference in binding affinity. Additionally, this C-terminal hydrophobicity appears to be critical for the weak binder but not for the tight binder. This prompted us to ask the following questions. What contributes to the binding affinity of SCGF for the PSMD9 PDZ domain? What limits the binding affinity of GRRF? Finally, is it possible to characterize the role of each residue in binding to enable the conversion of the poor binding GRRF to a tight binder, which could compete more effectively with its natural counterpart in hnRNPA1, thereby inhibiting PSMD9–hnRNPA1 interactions?

MATERIALS AND METHODS

Cloning, Expression, and Purification of the PDZ Domain. The PDZ domain was amplified from the PSMD9-pRSETA plasmid and cloned in the His-tagged expression vector, pETyong, between *Bam*HI and *Eco*RI restriction sites. For protein expression, a single colony of PDZ-pETyong in BL21 Codon Plus cells (Agilent) was inoculated in 5 mL of Luria broth with 50 μg/mL kanamycin and 34 μg/mL chloramphenicol. The overnight starter culture was inoculated in 1 L of LB kanamycin/chloramphenicol medium, and the culture was allowed to grow until the OD reached 0.4, after which isopropyl β-D-1-thiogalactopyranoside was added to a final concentration of 100 μM. The culture was grown until the OD reached 1.5. Cells were harvested by centrifugation at 5000 rpm. The induced cell pellet was resuspended in lysis buffer [50 mM Tris (pH 7.5), 150 mM NaCl, 10 mM imidazole, 0.1% Triton X-100, 10% glycerol, 5 mM β-mercaptoethanol, and 1× protease inhibitor]. Purification of the PDZ domain was carried out by nickel affinity (Ni-IDA) chromatography (Clontech, Takara) followed by gel filtration chromatography on a HiLoad 16/600 Superdex200 column (GE Healthcare).

Peptide Synthesis and Purification. Peptides were commercially synthesized from APS Lifetech. Peptides were synthesized with N-terminal biotin tag (Biotin-KGG-XXXX-OH, where XXXX corresponds to the peptide sequence and -OH is the carboxy terminus) and purified to 99% purity by high-performance liquid chromatography. Lyophilized peptides were reconstituted to give a concentration of 25 mM in 100% dimethyl sulfoxide (DMSO) (molecular biology grade, Sigma), dispensed in 10 μL aliquots, and stored at −20 °C. Cysteine-containing peptides were stored in DMSO containing 1 mM dithiothreitol.

Site-Directed Mutagenesis. Amino acid substitutions were carried out by site-directed mutagenesis using a modified protocol from the Stratagene QuikChange mutagenesis kit. Complementary primers were synthesized, each carrying the mutation in the center, flanked on both sides by unmodified nucleotide sequence (described in Table S1). The polymerase chain reaction-amplified products were subjected to DpnI digestion to remove parental DNA and transformed in *Escherichia coli* DH5α cells. Plasmids were isolated using the plasmid isolation kit (Sigma GenElute kit) and sequenced (Eurofins Genomics India Pvt Ltd.).

An Enzyme-Linked Immunosorbent Assay (ELISA) for Protein–Peptide Interaction and Inhibition of Protein–Protein Interaction. An ELISA for protein–peptide interaction and inhibition of protein–protein interaction was performed as described previously.[7]

5,5′-Dithiobis(2-nitrobenzoic acid) (DTNB) Labeling of Protein. The purified PDZ domain (72 μM) was incubated with a 20-fold molar excess (1440 μM) of DTNB ((Invitrogen) or Ellman's reagent[8] in 50 mM Tris and 150 mM NaCl (pH 8.5) for 1 h at 25 °C in the dark. DTNB reacts with the free thiol, converting it to 2-nitro-5-thiobenzoate (TNB^-), which is ionized to TNB^{2-} dianion, a yellow-colored compound. The excess DTNB was removed by desalting over a PD10 desalting column (G25 Sephadex, GE Healthcare). The absorption spectrum of the labeled protein was monitored from 280 to 700 nm, and the extent of labeling was calculated from the absorbance at 412 nm and the molar extinction coefficient of DTNB.

Glutathione Modification of Protein. The purified PDZ domain was incubated with a 20-fold molar excess of glutathione in 50 mM Tris and 150 mM NaCl (pH 8.5) for 1 h. The excess unreacted glutathione was removed by desalting over a PD10 column (G25 Sephadex, GE Healthcare). The extent of glutathione modification was checked by incubation of the glutathione-modified PDZ domain with an excess of DTNB, which would react with free cysteines, if available, and monitoring the absorption spectrum from 280 to 700 nm.

Homology Modeling. There is currently no crystal structure available for the PDZ domain of PSMD9 protein. Hence, the three-dimensional atomic structure of this domain was constructed using comparative modeling methods using the program Modeler (version 9.12) as described previously.[7] The sequence used for modeling of the PDZ domain of PSMD9 and the corresponding secondary structural regions are highlighted (Figure 3). The sequences of Nas2 and PSMD9 are 42% identical and 64% similar in their PDZ domains. The crystal structure of the Nas2 PDZ domain from yeast [Protein Data Bank (PDB) entry 4OO6],[9] the ortholog of mammalian PSMD9, was used as the template for modeling the PDZ domain of PSMD9.

Peptide Docking. The three-dimensional (3D) structures of the PDZ–GRRF and PDZ–SCGF complexes were generated as described previously.[7] Using the same protocol, 3D models of PDZ complexed with variants of GRRF and SCGF peptides were generated. The 3D structures of the linear conformations of the peptides were generated using the Xleap module in AMBER 16.[10] The fully extended peptide was energy minimized in implicit solvent using the Sander module in AMBER 16. Then, the minimized peptide in its extended conformation was docked with the refined model of the PDZ domain of PSMD9 protein. Peptide docking was carried out with two different docking programs, HADDOCK[11] and ATTRACT.[12,13] For the docking of peptides into the canonical

DOI: 10.1021/acs.biochem.9b00308
Biochemistry XXXX, XXX, XXX–XXX

pocket of PDZ using HADDOCK, a binding site was defined using residues Gly215, Cys216, Asn217, Ile218, and Gln181 based on the available crystallographic data of other PDZ−peptide complexes. No such constraints were used for running ATTRACT (complete blind docking was performed).

Molecular Dynamics (MD) Simulations. MD simulations were carried out on the apo-PDZ domain and the modelled PDZ−peptide complexes. In addition, MD simulations were carried out for several PDZ mutant peptide complexes; the mutated peptide structures were generated by replacing (mutating) the respective residues in Pymol.[14] The Xleap module was used to prepare the system for the MD simulations. Hydrogen atoms were added, and the N-terminus of the GRRF peptide was capped with the residue ACE. All of the simulation systems were neutralized with appropriate numbers of counterions. The neutralized system was solvated in an octahedral box with TIP3P[15] water molecules, leaving at least 10 Å between the solute atoms and the borders of the box. MD simulations were carried out with the pmemd.cuda module of the AMBER 16 package in combination with the ff14SB force field.[16] All MD simulations were carried out in explicit solvent at 300 K. During all of the simulations, the long-range electrostatic interactions were treated with the particle mesh Ewald[17] method using a real space cutoff distance of 9 Å. The settle[18] algorithm was used to constrain bond vibrations involving hydrogen atoms, which allowed a time step of 2 fs during the simulations. Solvent molecules and counterions were initially relaxed using energy minimization with restraints on the protein and peptide atoms. This was followed by unrestrained energy minimization to remove any steric clashes. Subsequently, the system was gradually heated from 0 to 300 K using MD simulations with positional restraints (force constant of 50 kcal mol^{-1} $Å^{-2}$) on protein and peptides over a period of 0.25 ns, allowing water molecules and ions to move freely followed by gradual removal of the positional restraints and a 2 ns unrestrained equilibration MD simulation at 300 K. The resulting systems were used as starting structures for the respective production phase of the MD simulations. For each case, three independent (using different initial random velocities) MD simulations were carried out starting from the well-equilibrated structures. Each MD simulation was carried out for 100 ns, and conformations were recorded every 4 ps. Simulation trajectories were visualized using VMD,[19] and figures were generated using Pymol.[14]

MMPBSA Calculations. The MMPBSA (Molecular Mechanics Poisson−Boltzmann Surface Area) methodology has been widely used to investigate the docking of ligands to receptors.[20−22] We applied it to calculate the binding free energies between the PDZ domain and peptides. Five thousand conformations were extracted from the last 50 ns of the MD simulations of each PDZ−peptide complex. The MMPBSA calculations were carried out after removing the water molecules and the counterions. Binding free energies were calculated using the single trajectory method, based on the assumption that the bound and unbound conformations of the protein and peptide are quite similar. In this protocol, the isolated conformations of the peptide and the PDZ domain were extracted from the corresponding PDZ−peptide complexes. For each conformation, the binding free energy (ΔG_{bind}) for binding of the peptide to the protein was calculated as follows:

$$\Delta G_{bind} = G_{complex} - (G_{receptor} + G_{peptide}) \quad (1)$$

The binding free energy is estimated as a sum of three terms:

$$\Delta G_{bind} = \Delta G_{MM} + \Delta G_{sol} - T\Delta S \quad (2)$$

where ΔG_{MM} is the change in molecular mechanics energy upon complexation in the gas phase, ΔG_{sol} is the change in solvation free energy, and $T\Delta S$ is the change in conformational entropy associated with ligand binding. The entropy term ($-T\Delta S$) was not computed and hence not included in the binding energy values.

The molecular mechanics free energy (ΔG_{MM}) is further split into van der Waals (ΔG_{vdw}) and electrostatic (ΔG_{ele}) energies:

$$\Delta G_{MM} = \Delta G_{ele} + \Delta G_{vdw} \quad (3)$$

Solvation free energy ΔG_{sol} arises from polar (electrostatic) solvation free energy (ΔG_{PB}) and nonpolar solvation free energy (ΔG_{SA}) as in eq 4:

$$\Delta G_{sol} = \Delta G_{PB} + \Delta G_{SA} \quad (4)$$

ΔG_{PB} is computed by solving the linearized Poisson−Boltzmann (PB) equation using Parse radii and a solvent probe radius of 1.4 Å. In our calculations, the dielectric constant was set to 1.0 for the interior of the solutes and 80.0 for the solvent. ΔG_{SA} was determined using a solvent accessible surface area (SASA)-dependent term as in eq 5:

$$\Delta G_{SA} = \gamma \times \mathrm{SASA} + \beta \quad (5)$$

where γ is the surface tension proportionality constant and was set to 0.00542 kcal mol^{-1} $Å^{-2}$ and β is the offset value, which was set to 0.92 kcal/mol here.

Per-Residue Decomposition. To detect the "hot spot" residues, the effective binding energies were decomposed into contributions of individual residues using the MMGBSA energy decomposition scheme. The MMGBSA calculations were carried out in the same way as in the MMPBSA calculations. The polar contribution to the solvation free energy was determined by applying the Generalized Born (GB) method (igb = 2),[42] using mbondi2 radii. The nonpolar contributions were estimated using the ICOSA method[42] by a SASA-dependent term using a surface tension proportionality constant of 0.0072 kcal mol^{-1} $Å^{-2}$.

RESULTS

The PDZ Domain Is the C-Terminal Peptide Recognition Domain in PSMD9. In our previous study,[7] we had generated a structural model of the PDZ domain of PSMD9 (as there was no structural data available) using the solution nuclear magnetic resonance (NMR) structure of the PDZ2 domain of harmonin (PDB entry 2KBS with the bound peptide) as the template;[23] the sequence of the PDZ domain of PSMD9 was 33% identical and 55% similar to that of PDZ2, the highest level of sequence identity among all of the PDZ domains with resolved structures at that time. The domain boundaries of the PDZ domain of PSMD9 predicted from this model lie between residues 108 and 195, similar to the annotation found in UniProt (O00233). However, the construct of the PDZ domain generated using these domain boundaries failed to express in *E. coli*. Later, the crystal structure of the Nas2 PDZ domain from yeast, the ortholog of mammalian PSMD9, was reported (PDB entry 4OO6).[9] Using this structure as a template, we revisited the domain

DOI: 10.1021/acs.biochem.9b00308
Biochemistry XXXX, XXX, XXX−XXX

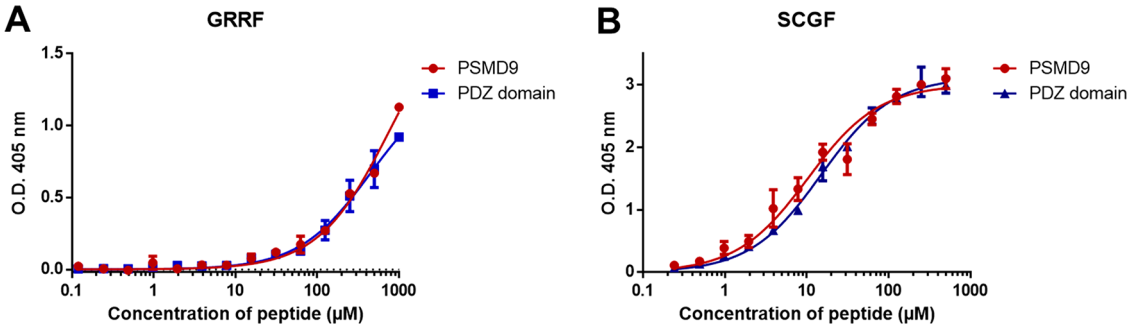

Figure 1. Comparison of the binding affinities of C-terminal peptides for PSMD9 and the PDZ domain. The interaction of PSMD9 and the PDZ domain with C-terminal tetrapeptides GRRF (C-terminus of hnRNPA1) (A) and SCGF (C-terminus of growth hormone) (B) was tested by an ELISA. The dissociation constant was calculated to be 758.2 ± 116.2 μM for the PSMD9−GRRF interaction and 439.3 ± 62.94 μM for the PDZ domain−GRRF interaction. The dissociation constant was calculated to be 10.30 ± 1.35 μM for the PSMD9−SCGF interaction and 11.06 ± 0.75 μM for the PDZ domain−SCGF interaction. Data were collected for a sample run in duplicate and represented as mean ± SEM [standard error of the mean (n = 2)]. The data were fit to a one-site-specific binding model in GraphPad Prism software.

boundaries of the PDZ domain of PSMD9 and designed a new construct of the PDZ domain spanning residues 121−223. This PDZ domain was found to be soluble, was expressed in a stable form, and could be purified to homogeneity (Figure S1). We tested the ability of the isolated PDZ domain to bind to the two differential binders, the GRRF and SCGF tetrapeptides identified earlier during screening.[7] Like full-length PSMD9, the PDZ domain was found to bind to GRRF with a low affinity (K_D = 439.3 ± 62.94 μM) and to SCGF with a high affinity (K_D = 11.06 ± 0.75 μM); additionally, the affinities were remarkably close to those observed with full-length PSMD9 (Figure 1A,B). These results indicate that the PDZ domain essentially accounts for the entire C-terminal peptide binding potential of PSMD9.

Designing a Super Binding Peptide. As described in the introductory section, the high-affinity interaction of SCGF and the inability of SGGF but not the SCGG mutant peptide to inhibit the growth hormone−PSMD9 interaction implied a hitherto unreported role of the cysteine at the P−2 position in defining the binding affinity of the SCGF peptide. We, therefore, asked whether replacing the arginine at the P−2 position in GRRF with cysteine would convert the low-affinity sequence (GRRF) to a tight binding motif GCRF. Indeed, peptide GCRF (K_D = 5.66 ± 0.62 μM) bound with an almost 100-fold greater affinity than GRRF, and the affinity was marginally better than that of SCGF (Table 1). In addition, replacing cysteine at the P−2 position in peptide SCGF to give SGGF resulted in the complete abrogation of peptide binding (Table 1), emphasizing the importance of cysteine at the P−2 position in imparting a high affinity for the peptide to the PDZ domain of PSMD9. Thus, with the newly engineered soluble PDZ domain, and design guided by experimental data, we converted a very weak binding peptide (GRRF) to a tight binder (GCRF) and identified a unique position-specific determinant that confers high affinity to the peptide that binds the PSMD9 PDZ domain.

Noncovalent Nature of the PDZ Domain−SCGF Motif Interaction. The binding experiments with designed peptide variants suggested that the presence and precise positioning of cysteine in the peptides can drive high-affinity interactions and can be used to generate tight binding peptides. Because the free thiol group of cysteine has the propensity to form a disulfide bond with a neighboring cysteine, we tested the possibility that the high affinity of the cysteine peptides for the PSMD9 PDZ domain may be due to the formation of a disulfide bond between the cysteine residue in the peptide and the cysteine residue of the PDZ domain. In our structural model, the β5 sheet that forms the floor for the peptide interactions harbors a cysteine (Cys216). We modified this singular cysteine by reaction with Ellman's reagent, DTNB. Approximately 80% of the PDZ domain was modified at the end of 2 h incubation. This modification had no effect on the binding affinity of SCGF (K_D = 11.06 ± 0.75 μM for the wild-type PDZ domain, and K_D = 7.5 ± 0.66 μM for the thiol-modified PDZ domain) (Table 1). In addition, we mutated the cysteine in the PDZ domain to a glycine (C216G) and found that the mutation did not alter peptide binding (K_D = 12.86 ± 0.99 μM) (Table 1). Together, these results provide unambiguous evidence underscoring the role of cysteine in driving high-affinity interaction of the peptides with the PSMD9 PDZ domain through noncovalent interactions.

Table 1. Binding Affinities of C-Terminal Peptide Variants for Wild-Type, Modified, and Mutant PDZ Domains[a]

peptide	protein	K_D (μM) ± SEM (n = 2)
GRRF	PDZ WT	439.3 ± 62.94
SCGF	PDZ WT	11.06 ± 0.75
GCRF	PDZ WT	5.66 ± 0.62
GRRC	PDZ WT	71.65 ± 9.05
SCGG	PDZ WT	44.03 ± 7.19
SGGF	PDZ WT	no binding
GCGF	PDZ WT	8.89 ± 0.82
SCGF	C216G mutant of the PDZ domain	12.86 ± 0.99
SCGF	F162G mutant of the PDZ domain	19.9 ± 0.71
SCGF	Q181G mutant of the PDZ domain	17.24 ± 1.07
SCGF	I218G mutant of the PDZ domain	21.45 ± 2.03
SCGF	glutathione-modified PDZ domain	9.94 ± 0.64
SCGF	DTNB-modified PDZ domain	7.5 ± 0.66
GCRF	DTNB-modified PDZ domain	13.4 ± 1.17

[a]Data were computed from a one-site-specific binding model using GraphPad Prism software.

Inhibition of Protein−Protein Interaction by Designed Peptides. Once we defined a tight binder of the PSMD9 PDZ domain, we investigated whether this motif could inhibit the interaction of PSMD9 with hnRNPA1. Both SCGF and GCRF inhibited PSMD9−hnRNPA1 interaction. The IC_{50} values were found to be 3.4 μM for GCRF (Figure 2), which is very similar to that of SCGF (5.5 μM) but several-fold more potent than that of the parent peptide GRRF (758.2

DOI: 10.1021/acs.biochem.9b00308
Biochemistry XXXX, XXX, XXX−XXX

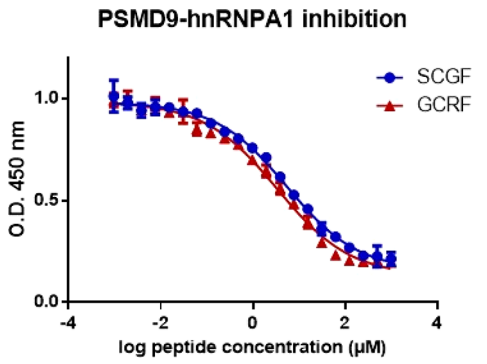

Figure 2. Inhibition of PSMD9−hnRNPA1 interaction by C-terminal peptides SCGF (blue) and GCRF (red). The IC_{50} values of SCGF and GCRF were 5.5 and 3.4 μM, respectively. Data were collected from a sample run in duplicate and are represented as mean ± SEM (n = 2). The data were fitted to a dose−response curve for inhibition with a variable slope (four parameters) in GraphPad Prism software.

μM).[7] We next aimed to understand the structural basis for these differences in the affinities of the various peptides. This information would inform future strategies for the design of peptide mimetics or small molecule inhibitors of IκBα degradation and NF-κB signaling, via inhibition of the PDZ domain of PSMD9.

Homology Model of the PSMD9 PDZ Domain. Equipped with the successful demonstration of the near complete overlap between peptide binding to PSMD9 and the engineered PDZ domain, homology models were generated using the Nas2 PDZ domain (~42% identity and 64% similarity in sequence) structure as a template; this contrasts with the older model,[23] in which the solution NMR structure of the PDZ2 domain of harmonin was used as the template. The model adopts a fold consisting of five β-sheets and two α-helices (Figure 3A). The peptide binding pocket is very similar in both models, except that in the new model the floor of the binding groove is now formed by the β5 sheet instead of the typical β2 sheet observed in most PDZ domain structures[3] (Figure S2). The binding site is primarily hydrophobic and is complemented by a small positive potential, arising from a charge cluster located at one end of the binding groove (Figure 3B). A detailed comparison of the old and new homology models of PSMD9 is discussed in the Supporting Information (Figure S3)

Ligand Mapping MD Simulations. The homology model was subjected to all-atom MD simulations. These show that the overall structure of the apo PDZ domain was stable with a root-mean-square deviation (RMSD) of ~4.5 Å (Figure 4A). The α2 helix that is part of the α/β binding groove is flexible in the apo state (Figure 4B,C), resulting in deformations and instabilities in the α/β binding pocket. The binding site adopts a closed conformation with both the α-helix (α2) and the β-strand (β5) assuming a collapsed state (Figure 4D) to occlude the "active site" residues as can be seen from the decreased distance between α2 and β5 (Figure 4D). To open this hydrophobic pocket, we decided to carry out ligand mapping simulations, which are techniques for enhancing sampling and access to buried/cryptic pockets.[25,26] These simulations were carried out with benzene molecules added to the solvent. No unfolding of the PDZ domain was observed during the ligand mapping simulations (Figure S4). As suggested, the benzene molecules occupy the hydrophobic peptide binding groove, preventing the formation of the closed state. Additionally, the presence of the benzene molecules in the peptide binding groove also resulted in a widening of the groove by ~3 Å as compared to that of the standard MD simulations of the apoprotein (Figure 4D) in an aqueous environment. In addition, the conformations sampled were clustered to identify conformational "substates" that we use for docking the peptides.

Docking of GRRF and SCGF Peptides to the PDZ Domain. For PDZ domain−peptide docking, two different docking algorithms/programs (Haddock and ATTRACT) were used. Both programs predicted that both of the peptides, GRRF and SCGF, would bind at the binding groove between helix α2 and sheet β5 of the PDZ domain (Figure 5). Upon visual inspection of all the docked poses, a peptide−protein complex similar to PDZ−peptide complexes[3] with phenylalanine at the P0 position was chosen. In this conformation, the peptide binds in an extended manner, antiparallel to sheet β5, and engages in a large number of polar and hydrophobic interactions that extend the β-sheet by an additional strand (Figure 5) as seen with a typical PDZ domain−C-terminal peptide interaction. The hydrophobic side chain of phenyl-

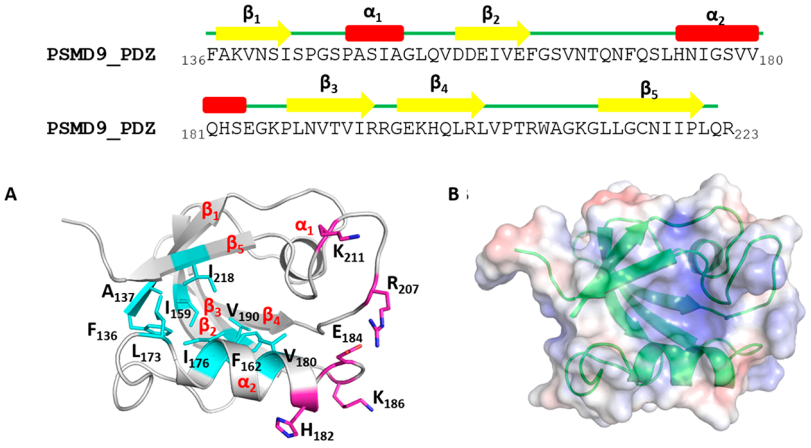

Figure 3. Sequence of the PDZ domain of PSMD9 with secondary structures mapped. (A) Cartoon representation. (B) Electrostatic surface representation calculated using APBS,[24] in which the blue and red refer to positive (5 kcal/mol) and negative (−5 kcal/mol) potentials, respectively, of the homology model of the PDZ domain of PSMD9.

DOI: 10.1021/acs.biochem.9b00308
Biochemistry XXXX, XXX, XXX−XXX

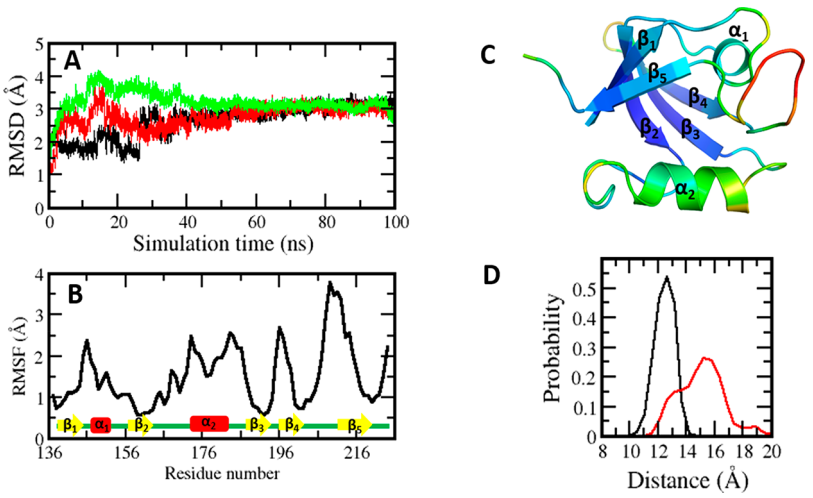

Figure 4. (A) RMSD (black, red, and green correspond to three triplicates). RMSD was calculated by superimposing all the residues of the sampled structures onto the starting structure of the simulation. (B) Root-mean-square fluctuation of the conformations of the PDZ domain of PSMD9 in its apo state. (C) Cartoon representation of the apo PDZ domain colored according to flexibility, with blue to red corresponding to low to high flexibility, respectively. (D) Distance between the α2 helix and β5 sheet in the binding groove of the conformations sampled during apo (black) and ligand mapping (red) simulations.

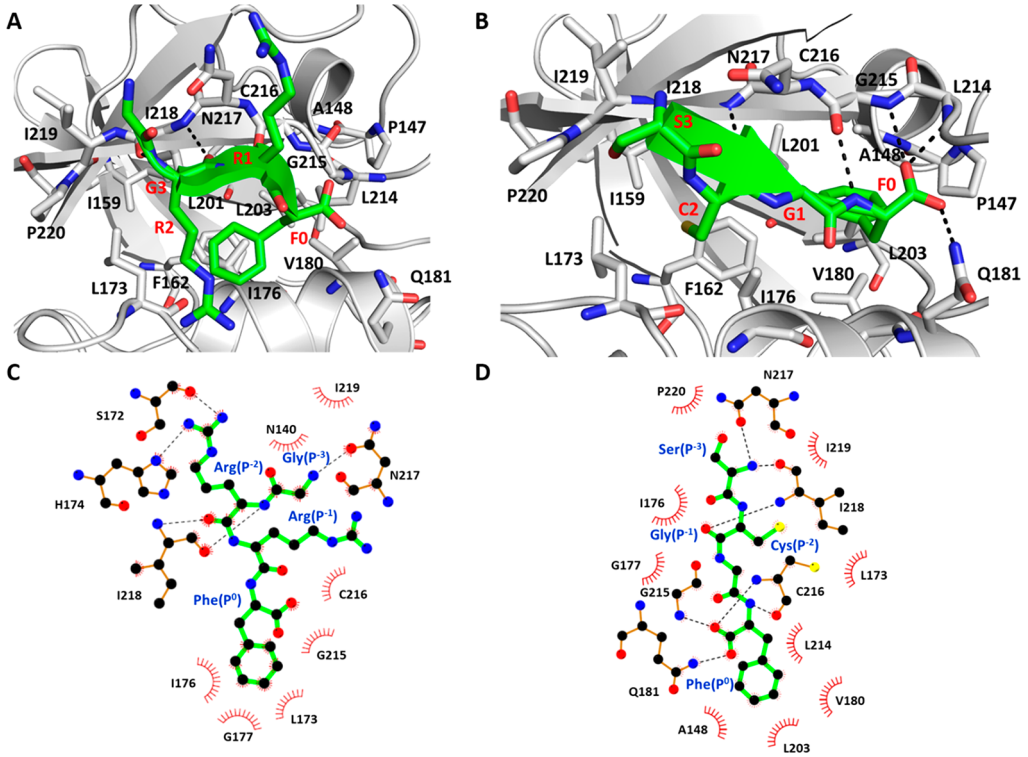

Figure 5. Cartoon representation of the PDZ domain of PSMD9 in complex with the (A) GRRF and (B) SGCF peptides. Important residues in the binding site are shown as sticks. The peptide is bound in canonical mode and shown as sticks (labeled in red). Hydrogen bonds are highlighted with black dashed lines. (C and D) Two-dimensional diagrams of PDZ domain−peptide [(C) GRRF and (D) SCGF] residue contacts calculated using Ligplot.[28]

alanine at the P0 position of the peptide buries into the hydrophobic pocket formed by Pro147, Ala148, Phe162, Ile176, Val180, Leu201, Leu203, Gly215, and Cys216 (Figure 5). The peptide further interacts with the β-sheet mainly through backbone/side chain hydrogen bonds with residues Gly215, Cys216, Asn217, and Ile218 of strand β5 of the PDZ domain (Figure 5). Some of these interactions were similar to those proposed for the interactions of Nas2 with the C-terminus of the archaeal ATPase.[27]

Molecular Dynamics Simulations of PDZ Domain−Peptide Complexes. To evaluate the stability of the predicted binding mode of the GRRF and SCGF peptides, the PDZ domain−peptide complexes were subjected to MD simulations. The overall structure of the protein−peptide docked models remained stable, with both the protein and the peptide remaining bound within an RMSD of ~4 Å against the docked models (Figure 6A,B). In these complex simulations, the PDZ domain displayed reduced flexibility, as the presence

DOI: 10.1021/acs.biochem.9b00308
Biochemistry XXXX, XXX, XXX−XXX

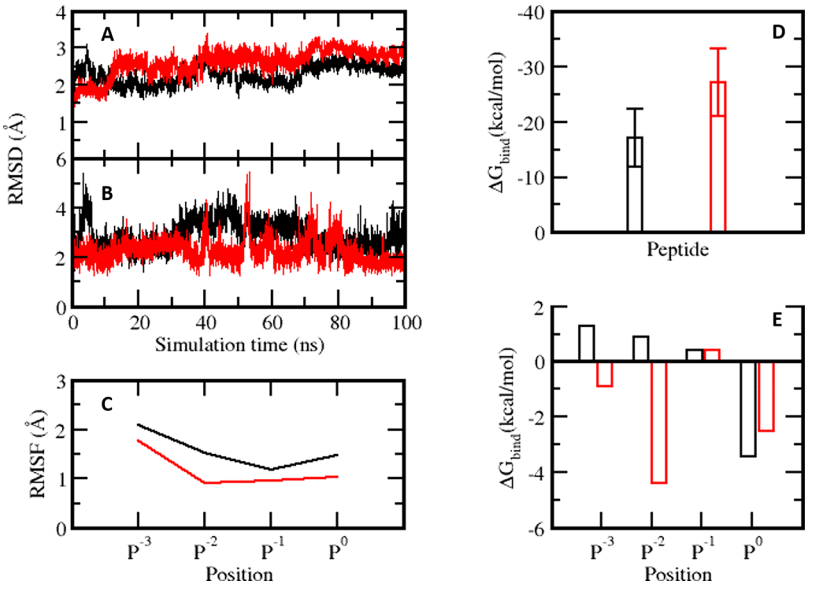

Figure 6. RMSD (RMSD calculated by superimposing all the residues of the sampled structures onto the starting structure of the simulation) of (A) the peptide-bound PDZ domain and (B) the bound peptide. (C) Root-mean-square fluctuation of the conformations of GRRF (black) and SCGF (red) peptides in complex with PDZ, from the corresponding complex simulations. (D) Calculated MMPBSA binding free energies (ΔG_{bind}) for PDZ−GRRF (black) and PDZ−SCGF (red) complexes. (E) Decomposition of the binding free energy on a per-residue basis for all four residues in the GRRF (black) and SCGF (red) peptides from the corresponding complex simulations.

of the peptide stabilizes the binding groove and the nearby loop, attenuating the conformational flexibility seen in the apo PDZ domain. The peptide in its bound state was stabilized by various interactions and also shows reduced flexibility, with the N-terminal region being wobbly as compared to the C-terminal region (Figure 6C). The C-terminal phenylalanine of the peptide remains deeply buried in SCGF but partially buried in GRRF within a hydrophobic crevice located at one end of the $\alpha2-\beta5$ binding groove (Figure 5). The peptides further interact with the terminal $\beta5$ sheet mainly through backbone/side chain hydrogen bonds with residues Gly215, Cys216, Asn217, and Ile218 of strand $\beta5$ and Gln181 from helix $\alpha2$ of the PDZ domain (Figure 5A,B). In the case of SCGF, the P−2 cysteine (i.e., second from the N-terminus, third from the C-terminus) occupies the hydrophobic binding pocket (formed by Ile159, Phe162, Leu173, Ile176, and Ile218) and the shorter hydrophobic side chain of the P−2 cysteine remains buried in the pocket. In contrast, the side chain of the arginine at the P−2 position in the GRRF peptide does not occupy the binding pocket and is exposed to solvent, interacting with helix $\alpha2$. The longer side chain of the P−2 arginine further prevents the side chain of the P0 phenylalanine from being deeply buried in the hydrophobic pocket. The buried side chains of the P−2 cysteine and the P0 phenylalanine provide tight packing for the bound SCGF peptide, which is not possible in the case of GRRF due to the tendency of the P−2 arginine to remain exposed to the solvent. This is further evident from the analysis of the interaction of PDZ−GRRF and PDZ−SCGF complexes. In the case of the PDZ−SCGF complex, the backbone of the bound peptide is involved in five hydrogen bond interactions with the backbone of strand $\beta5$, with three of these hydrogen bonds (N217−C2, C216−F0, and G215−F0) preserved for >90% of the simulation time and the other two (I218−S3 and Q181−F0) preserved for ∼50% of the simulation time. However, in the PDZ−GRRF complex, only three backbone−backbone hydrogen bond interactions were observed between the peptide and PDZ, only one interaction (I218−R2) being long-lived (75% of the simulation time), while the other two hydrogen bonds (I218−G3 and C216−F0) were less stable (<40% of the simulation time). The considerable differences in the number of bonds formed and the extent of tight packing of peptides SCGF and GRRF with PDZ could readily account for their dramatically different binding affinities. In summary, MD simulations provide a plausible model underlying the observed differences in affinity between the SCGF and GRRF peptides and a likely role of the P−2 arginine (vis-à-vis cysteine) that was not evident from the biochemical experiments.

Determination of the Binding Affinity of PDZ−Peptide Complexes. We next analyzed the energetics of interactions of the peptide with the PDZ domain. In general, the energies of interaction of the peptides with the PDZ domain are favorable (ΔG between −17.5 and to −27.2 kcal/mol) (Figure 6D); however, the SCGF peptide showed better binding (ΔG = −27.2 kcal/mol) compared to that of GRRF (ΔG = −17.5 kcal/mol). This is in good agreement with the experimental data (the K_D of GRRF is ∼440 μM, and the K_D of SCGF is ∼11 μM). Further analysis from the models revealed that the P0 phenylalanine makes a significant contribution to the binding of both peptides, more so in the case of GRRF (as seen in experiments), highlighting the importance of hydrophobicity (Figure 6E). In the case of GRRF, the rest of the peptide residues do not contribute favorably to the binding free energy. In contrast, all of the residues of SCGF contribute favorably to its binding, with the P−2 cysteine making significant contributions [$\Delta G \sim -4.5$ kcal/mol (Figure 6E)]. From the PDZ domain, only residues from the $\alpha2-\beta5$ binding groove appear to contribute to the binding energetics, with the major contributions [$\Delta G \leq -3.0$ kcal/mol (Figure S5)] coming from the residues of strand $\beta5$ (Figure S5).

Deciphering the Role of C-Terminal Hydrophobicity in Mediating Affinity. Extensive structural studies have indicated that binding of a peptide to PDZ domains is mediated predominantly by the four terminal residues of the

DOI: 10.1021/acs.biochem.9b00308
Biochemistry XXXX, XXX, XXX−XXX

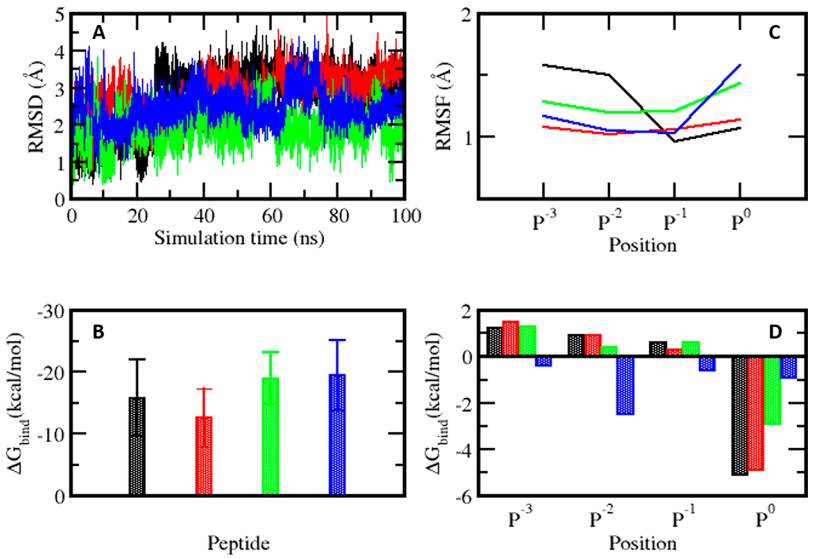

Figure 7. (A) RMSD (RMSD calculated by superimposing all the residues of the sampled structures onto the starting structure of the simulation) of the bound peptide. (C) Root-mean-square fluctuations of the conformations of GRRL (black), GRRI (red), GRRC (green), and SCGG (blue) peptides in complex with PDZ, from the corresponding complex simulations. (B) Calculated MMPBSA binding free energies (ΔG_{bind}) for PDZ−peptide complexes. (D) Decomposition of the binding free energy on a per-residue basis for all four residues in the GRRL (black), GRRI (red), GRRC (green), and SCGG (blue) peptides from the corresponding complex simulations.

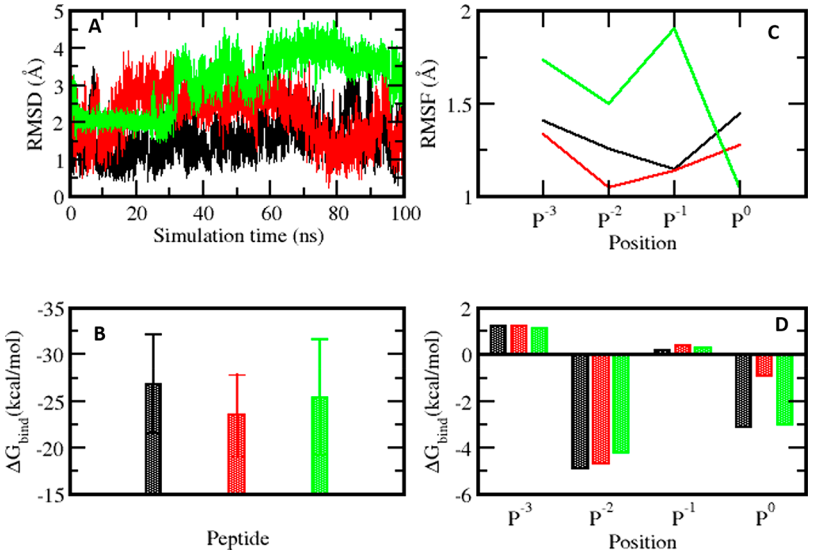

Figure 8. (A) RMSD (RMSD calculated by superimposing all the residues of the sampled structures onto the starting structure of the simulation) of the bound peptide. (C) Root-mean-square fluctuations of the conformations of GCRF (black), GCRG (red), and GCGF (green) peptides in complex with the PDZ domain from the corresponding complex simulations. (B) Calculated MMPBSA binding free energies (ΔG_{bind}) for PDZ-peptide complexes (D) Decomposition of the binding free energy on a per-residue basis for all four residues in the GCRF (black), GCRG (red), and GCGF (green) peptides from the corresponding complex simulations.

peptide that interact directly with the binding groove in the PDZ domains.[29] As mentioned above, the binding groove in the PSMD9 PDZ domain is unusual and is characterized by a cyclic permutation in which sheet β5 forms the floor instead of sheet β2. Therefore, to understand whether the conserved mode of interaction, especially of the P0 hydrophobic residues, is affected due to an altered β-sheet arrangement, we undertook an extensive analysis of the peptide−PDZ complex. In the simulations, peptides GRRL, GRRI, and GRRC, all with a hydrophobic residue at the C-terminus, remain stably bound to PDZ with an RMSD of <4 Å (Figure 7A) and the C-terminal leucine, isoleucine, and cysteine at the P0 position are buried in the hydrophobic pocket. As with GRRF, the bound peptides show reduced flexibility, with the C-terminal region showing decreased flexibility as compared to the N-terminal region (Figure 7C). Peptide−protein backbone interactions (I218−G3, C216−I0/C0/C0, and I218−R2) stabilize the bound state of the peptide and the PDZ domain (preserved for ∼75% of the simulation time). If the side chain at the C-terminus is removed as in GRRG, the peptide unbinds from the canonical binding mode within ∼5−10 ns of the simulation (Figure S6). This unstable binding of the GRRG peptide is in agreement with experimental observations that show that when the P0 phenylalanine is mutated to glycine, the peptide no longer inhibits the PSMD9−hnRNPA1 interactions.[7]

DOI: 10.1021/acs.biochem.9b00308
Biochemistry XXXX, XXX, XXX−XXX

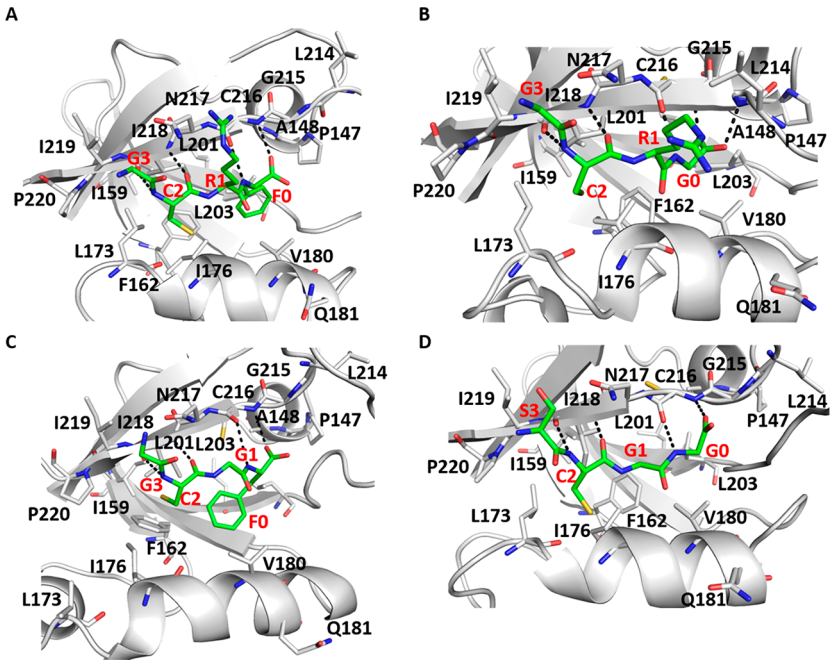

Figure 9. Snapshots from MD simulations of peptides (A) GCRF, (B) GCRG, (C) GCGF, and (D) SCGG bound to the PDZ domain from the corresponding complex simulations.

However, in sharp contrast to the unstable GRRG−PDZ complex, the SCGG peptide bound stably in the peptide binding groove with an RMSD of ∼3.0 Å during the simulations (Figure 7A). The bound SCGG peptide is involved in backbone−backbone interactions (N217−C2, C216−G0, G215−G0, I218−S3, and Q181−G0) with strand β5 of the PDZ domain; however, now the C-terminus of the peptide shows increased flexibility compared to the N-terminus probably because of two glycine residues located at the C-terminus. The stable binding of the SCGG peptide is in agreement with experimental observations in which the affinity of the SCGG peptide is ∼44 μM (Table 1).

Importance of the Cys at the P−2 Position for the Binding of Tetrapeptides (MD simulations). From the detailed analysis of the contributions of residues to the interactions of the peptides, it is obvious that C-terminal hydrophobicity is critical for the binding of at least the GRRX series of peptides but less so for the SCGX series. The residue at the P−2 position, i.e., arginine, in fact, disfavors binding in the case of the GRRX series, but the residue at this position in the SCGX series, i.e., cysteine, contributes significantly to the binding energy (Figure 6E). Therefore, we next investigated the importance of cysteine at the P−2 position for binding. Concomitant with our experimental data (Table 1), the SGGF peptide was less stable in our simulations, with the RMSD of the bound conformation reaching values as high as 7 Å (Figure S7). Although no complete unbinding of the peptide was observed during the MD simulation (the P0 phenylalanine remains buried in the pocket), the rest of the peptide moves away from the binding site, with no protein−peptide hydrogen bonds observed during the simulations.

Detailed MD simulations revealed that the P−2 cysteine contributes favorably to binding, while arginine at this position has a negative influence on the occupancy of the P0 phenylalanine. Together, these results explain how the replacement of arginine in GRRF with cysteine to yield GCRF results in increases in affinity (from 439 to 5.6 μM). Arginine has an inhibitory effect on the affinity of GRRF; the introduction of cysteine at this position mimics the effect seen in SCGF wherein cysteine at the P−2 position was found to contribute significantly [$\Delta G \leq -3.0$ kcal/mol (Figure 4)] to the binding energy. MD simulations revealed that the GCRF peptide remained stably bound with an RMSD of ∼3 Å (Figure 8A) with both the phenylalanine at the P0 position and cysteine at the P−2 position now buried in the binding pocket and the bound peptide stabilized by backbone−backbone hydrogen bond interactions (C216−F0, I218−C2, and I218−S3; stable for ∼90% of the simulation time) with strand β5 from the binding groove (Figure 9A). The tighter binding of the GCRF peptide is also mirrored in our energetic calculations; the ΔG of GCRF is −26.8 kcal/mol (Figure 8B), which is as good as that of SCGF with a ΔG of −27.2 kcal/mol (Figure 6D), while the ΔG of GRRF is only −17.5 kcal/mol (Figure 6D). As one can see with SCGF, the cysteine at the P−2 position makes significant contributions to the binding free energy (Figure 8D). The P−2 cysteine with a shorter side chain along with the side chain of the P0 phenylalanine is buried deep in the binding groove, enabling the peptide to be involved in stable hydrogen bond interactions with residues from strand β5 (Figure 9).

In a majority of PDZ−peptide complex structures tested here, neither glycine nor serine at the P−3 position of the peptide contributed significantly to the binding energy. For example, in peptide GCGF, ΔG for the P−3 glycine is approximately 1.5 kcal/mol (Figure 8D), and in peptides SCGF (Figure 6E) and SCGG (Figure 7D), the ΔG for the P−3 serine is approximately −1.5 kcal/mol. These values are within the error of the calculations. We also evaluated the contribution of the P−3 residue to the binding affinity by testing the GCGF peptide, a variant of the SCGF peptide (with glycine at the P−3 position instead of serine). The affinity of GCGF for the PDZ domain (K_D = 8.89 ± 0.82 μM) was almost identical to that of the SCGF peptide (K_D = 11.06 ± 0.75 μM) (Table 1). These results indicate that cysteine is

DOI: 10.1021/acs.biochem.9b00308
Biochemistry XXXX, XXX, XXX−XXX

the primary mediator for high-affinity interactions in these peptides, and serine has little or no effect. The positional occupancy of cysteine is also important in dictating maximal binding affinity because moving the cysteine from the P−2 position to the P0 position as in GRRC improved the affinity by only 5-fold (72 μM for GRRC vs 439 μM for GRRF) (Table 1).

Contribution of Residues in the Binding Pocket to Peptide Binding. The docking studies pinpointed crucial residues P147, A148, F162, I176, V180, L201, L203, G215, C216, N217, and I218 in the PDZ domain that contribute to the bulk of peptide binding energy. We investigated the contribution of three primary residues, F162 (β2), Q181 (α2), and I218 (β5), to peptide binding by mutating each of them to a glycine residue. All three mutations led to a modest decrease in affinity (Table 1), indicating the importance of these residues in peptide binding. These results are similar to those of single-amino acid substitutions made in the PDZ3 domain of PSD-95.[30] Besides modifying cysteine with DTNB (Table1), we also modified the PDZ domain by incubating it with glutathione. The unreacted glutathione was removed by desalting, and the PDZ domain was tested for interaction with the peptide. The peptide binding was unaffected (K_D = 9.94 ± 0.64 μM) (Table 1). These results indicate that Ile218 in strand β5 has a better contribution to the binding energy than Cys216.

DISCUSSION AND CONCLUSION

More than 250 nonredundant PDZ domains have been identified from 150 PDZ domain-containing proteins.[3] Despite a low level of sequence identity (<30%), the overall fold is conserved across the family with the variations localized largely to the loop regions.[31−33] The PDZ domain, like other protein-interacting domains such as SH3, WW, and SH2, mediates biological processes often through transient interactions involving small regions of the interacting partner. In accordance, these isolated domains often recognize short peptides with specific sequence motifs. The small nature of the binding surface combined with the specific and conserved nature of PDZ−peptide interactions makes the PDZ domains attractive "druggable" targets and have guided the rational design of several small molecules and peptide-based inhibitors.[34−36] In addition, peptide analogues or blockers that disrupt PDZ domain interactions have also been useful for understanding how these domains regulate functions of their interacting proteins.[37,38] While these results have been extremely encouraging, the low level of sequence conservation and the lack of extensive structural data on apo and peptide or protein-bound structures of the PDZ complexes remain major deterrents in exploiting these interactions exhaustively for designing novel inhibitors for blocking associated signaling cascades. This lacuna is considerably overcome by extremely detailed biochemical and biophysical investigations of the sequence determinants of binding that in some cases is accompanied by mutagenesis studies to identify per-residue contributions to binding affinity. Some of the major outcomes of these studies have been (a) the identification of the common determining factor for peptide recognition by the PDZ domains, which is a hydrophobic residue at the C-terminus of the peptide,[39] (b) the interaction that is typically governed by the binding of the C-terminus of an interacting peptide into a groove formed by a strand (β2) and a helix (α2) of the PDZ domain[3,40−42] leading to the interacting peptide assuming an antiparallel β-strand (relative to β2 of most PDZ domains), and (c) the P0 hydrophobic residue and the amino acid at the P−2 position that drive the bulk of binding energy in most of the known PDZ domains.

In this report, we pursue one such structure−activity relationship of the PDZ domain of PSMD9 and find that the hydrophobicity of the C-termini, which is the hallmark of peptide recognition by other PDZ domain proteins, does not fully account for the binding preference of the PSMD9 PDZ domain. The initial set of point mutations in PSMD9 peptide interactions underscores the requirement of hydrophobicity at the C-terminus of the peptide. Peptide binding is lost if the P0 phenylalanine in GRRF is mutated to glycine but retained if mutated to leucine (GRRL) or isoleucine (GRRI).[7] These observations are similar to those reported by other groups.[3,39−45] However, by investigating other peptide interactions with the PDZ domain, we found that the P0 hydrophobicity is not the primary driving force of the interaction; rather, an unusual noncovalent interaction via the cysteine residue at the P−2 position with the residues in strand β5 of the circularly permuted PDZ domain is a major affinity determinant (Table 1). Computational studies explain these experimental observations; classical hydrophobic residues such as phenylalanine can add to the affinity when the P−2 residue is a cysteine, as seen from the measurable loss of ΔG for binding when the phenylalanine at the P0 position is mutated in the high-affinity peptides or super binders.[7] On the basis of the modeled structures, one can envisage that in SCGG and GCRG peptides, the absence of phenylalanine generates an unfilled pocket, which is energetically unfavorable. Because the aromatic side chain of phenylalanine is involved in stacking interactions with other aromatic residues, it may play a significant role in the recognition of specific client proteins and hydrophobic ligands.[46]

Our simulations and energetic analyses also explain the complexity of the contributions of individual residues from the GRRX and SCGX series. Arginine at the P−2 position in the GRRX series contributed negatively to the binding free energy and is not favored in the richly hydrophobic and positively charged binding pocket, whereas in the case of SCGF and SCGG, the shorter and hydrophobic side chain of cysteine is well tolerated. The side chain of cysteine is buried deep in the pocket, while arginine is extruded into the solvent. The residue at the P−1 position in either series does not engage in side chain interactions and therefore does not dictate or influence specificity, similar to the observation made for other PDZ domains.[47] Similarly, the presence of serine or glycine at the P−3 position in the peptide does not influence binding affinity in the series tested here.

Thus, in conclusion, we report that C-terminal peptides, the sequences of which were derived from the C-termini of proteins, interact with the isolated PDZ domain of PSMD9. The domain contributed to the binding affinity of the full-length protein in its entirety, and the magnitude of binding is affected identically (full-length PSMD9 vis-à-vis the PDZ domain) by mutations in the peptide. The floor of the binding pocket that is occupied by strand β5 in the circularly permuted structure (as suggested by the model built on the basis of the Nas2 crystal structure) contributes to the interacting residues. A hitherto unidentified motif with cysteine occupying the P−2 position introduces a new class of binding preferences of the PDZ domains at large. So far, on the basis of ligand binding specificities, 16 distinct specificity classes of PDZ domains have

DOI: 10.1021/acs.biochem.9b00308
Biochemistry XXXX, XXX, XXX−XXX

been identified,[44] yet cysteine was not observed at the P−2 position as a strong contributor of affinity.

Collectively, our parallel in-depth biochemical, structure-guided modeling and robust MD simulations establish a unique signature motif in C-terminal peptides for high-affinity interactions with the PDZ domain of PSMD9 pinpointing position-specific positive and negative contributors of binding energy. The results led to the design of a super binding peptide GCRF, which is capable of inhibiting the PSMD9−hnRNPA1 interaction. The unique signature motif can be utilized as a scaffold for the design of peptide-based inhibitors for blocking signaling in cancers dependent on NF-κB for survival and chemo- and radiotherapy resistance.

■ ASSOCIATED CONTENT

Supporting Information

The Supporting Information is available free of charge on the ACS Publications website at DOI: 10.1021/acs.biochem.9b00308.

Additional experimental and computational results (PDF)

Accession Codes

PSMD9, UniProt entry O00233.

■ AUTHOR INFORMATION

Corresponding Authors

*E-mail: vprasanna@actrec.gov.in.
*E-mail: chandra@bii.a-star.edu.sg.

ORCID

Mahalakshmi Harish: 0000-0001-9547-3836
Srinivasaraghavan Kannan: 0000-0002-9539-5249
Mohan R. Pradhan: 0000-0001-9759-1676
Chandra S. Verma: 0000-0003-0733-9798

Present Address

#S.P.: Biological Sciences, University of Denver, 2199 S. University Blvd., Denver, CO 80208.

Author Contributions

¶Prasanna Venkatraman is the lead author.

Author Contributions

M.H. and S.K. contributed equally to this work. M.H. performed binding studies and wrote the manuscript. S.K. performed computational studies and wrote the manuscript. S.P. performed initial cloning and purification experiments. M.R.P. performed computational analysis. P.V. and C.S.V. conceived and directed the project and wrote and corrected the manuscript.

Funding

This project was funded by the Department of Biotechnology (DBT), Government of India (BT/PR21237/BRB/10/1550/2016), and an intramural grant, ACTREC (Project 258). M.H. acknowledges ACTREC [and an intramural grant (Project 258)] for a fellowship.

Notes

The authors declare no competing financial interest.

■ ACKNOWLEDGMENTS

The authors thank the National Super Computing Centre (NSCC) for computing facilities. The pETyong vector was a kind gift from Dr. Ruchi Anand, IIT Bombay.

■ ABBREVIATIONS

PDZ, PSD-95, Discs-large, ZO-I; PPIs, protein−protein interactions; hnRNPA1, heterogeneous nuclear ribonuclear protein A1; GH, growth hormone.

■ REFERENCES

(1) Kennedy, M. B. (1995) Origin of PDZ (DHR, GLGF) domains. *Trends Biochem. Sci. 20*, 350.
(2) Hung, A. Y., and Sheng, M. (2002) PDZ Domains: Structural Modules for Protein Complex Assembly. *J. Biol. Chem. 277*, 5699−5702.
(3) Lee, H.-J., and Zheng, J. J. (2010) PDZ domains and their binding partners: structure, specificity, and modification. *Cell Commun. Signaling 8*, 8.
(4) Tam, C. W., Cheng, A. S., Ma, R. Y. M., Yao, K.-M., and Shiu, S. Y. W. (2006) Inhibition of Prostate Cancer Cell Growth by Human Secreted PDZ Domain-Containing Protein 2, a Potential Autocrine Prostate Tumor Suppressor. *Endocrinology 147*, 5023−5033.
(5) Lin, E. Y. S., Silvian, L. F., Marcotte, D. J., Banos, C. C., Jow, F., Chan, T. R., Arduini, R. M., Qian, F., Baker, D. P., Bergeron, C., Hession, C. A., Huganir, R. L., Borenstein, C. F., Enyedy, I., Zou, J., Rohde, E., Wittmann, M., Kumaravel, G., Rhodes, K. J., Scannevin, R. H., Dunah, A. W., and Guckian, K. M. (2018) Potent PDZ-Domain PICK1 Inhibitors that Modulate Amyloid Beta-Mediated Synaptic Dysfunction. *Sci. Rep. 8*, 13438.
(6) Wang, N. X., Lee, H. J., and Zheng, J. J. (2008) Therapeutic use of PDZ protein-protein interaction antagonism. *Drug News Perspect. 21*, 137−141.
(7) Sangith, N., Srinivasaraghavan, K., Sahu, I., Desai, A., Medipally, S., Somavarappu, A. K., Verma, C., and Venkatraman, P. (2014) Discovery of novel interacting partners of PSMD9, a proteasomal chaperone: Role of an Atypical and versatile PDZ-domain motif interaction and identification of putative functional modules. *FEBS Open Bio 4*, 571−583.
(8) Ellman, G. L. (1959) Tissue sulfhydryl groups. *Arch. Biochem. Biophys. 82*, 70−77.
(9) Singh, C. R., Lovell, S., Mehzabeen, N., Chowdhury, W. Q., Geanes, E. S., Battaile, K. P., and Roelofs, J. (2014) 1.15 A resolution structure of the proteasome-assembly chaperone Nas2 PDZ domain. *Acta Crystallogr., Sect. F: Struct. Biol. Commun. 70*, 418−423.
(10) Case, D. A., Cerutti, D. S., Cheatham, T. E., III, Darden, T. A., Duke, R. E., Giese, T. J., Gohlke, H., Goetz, A. W., Homeyer, N., Izadi, S., Janowski, P., Kaus, J., Kovalenko, A., Lee, T. S., LeGrand, S., Li, P., Lin, C., Luchko, T., Luo, R., Madej, B., Mermelstein, D., Merz, K. M., Monard, G., Nguyen, H., Nguyen, H. T., Omelyan, I., Onufriev, A., Roe, D. R., Roitberg, A., Sagui, C., Simmerling, C. L., Botello-Smith, W. M., Swails, J., Walker, R. C., Wang, J., Wolf, R. M., Wu, X., Xiao, L., and Kollman, P. A. (2016) *AMBER 16*.
(11) Dominguez, C., Boelens, R., and Bonvin, A. M. (2003) HADDOCK: a protein-protein docking approach based on biochemical or biophysical information. *J. Am. Chem. Soc. 125*, 1731−1737.
(12) de Vries, S. J., Schindler, C. E., Chauvot de Beauchene, I., and Zacharias, M. (2015) A web interface for easy flexible protein-protein docking with ATTRACT. *Biophys. J. 108*, 462−465.
(13) Zacharias, M. (2003) Protein-protein docking with a reduced protein model accounting for side-chain flexibility. *Protein Sci. 12*, 1271−1282.
(14) Delano, W. L. (2002) *The PyMOL Molecular Graphics System*, DeLano Scientific, San Carlos, CA.
(15) Jorgensen, W. L., Chandrasekhar, J., Madura, J. D., Impey, R. W., and Klein, M. L. (1983) Comparison of simple potential functions for simulating liquid water. *J. Chem. Phys. 79*, 926−935.
(16) Maier, J. A., Martinez, C., Kasavajhala, K., Wickstrom, L., Hauser, K. E., and Simmerling, C. (2015) ff14SB: Improving the Accuracy of Protein Side Chain and Backbone Parameters from ff99SB. *J. Chem. Theory Comput. 11*, 3696−3713.

DOI: 10.1021/acs.biochem.9b00308
Biochemistry XXXX, XXX, XXX−XXX

(17) Darden, T., York, D., and Pedersen, L. (1993) Particle mesh Ewald: An N·log(N) method for Ewald sums in large systems. *J. Chem. Phys. 98*, 10089−10092.
(18) Miyamoto, S., and Kollman, P. A. (1992) Settle: An analytical version of the SHAKE and RATTLE algorithm for rigid water models. *J. Comput. Chem. 13*, 952−962.
(19) Humphrey, W., Dalke, A., and Schulten, K. (1996) VMD: visual molecular dynamics. *J. Mol. Graphics 14*, 33−38.
(20) Hou, T., Wang, J., Li, Y., and Wang, W. (2011) Assessing the performance of the molecular mechanics/Poisson Boltzmann surface area and molecular mechanics/generalized Born surface area methods. II. The accuracy of ranking poses generated from docking. *J. Comput. Chem. 32*, 866−877.
(21) Homeyer, N., and Gohlke, H. (2012) Free Energy Calculations by the Molecular Mechanics Poisson-Boltzmann Surface Area Method. *Mol. Inf. 31*, 114−122.
(22) Wang, J., Hou, T., and Xu, X. (2006) Recent Advances in Free Energy Calculations with a Combination of Molecular Mechanics and Continuum Models. *Curr. Comput.-Aided Drug Des. 2*, 287−306.
(23) Pan, L., Yan, J., Wu, L., and Zhang, M. (2009) Assembling stable hair cell tip link complex via multidentate interactions between harmonin and cadherin 23. *Proc. Natl. Acad. Sci. U. S. A. 106*, 5575−5580.
(24) Baker, N. A., Sept, D., Joseph, S., Holst, M. J., and McCammon, J. A. (2001) Electrostatics of nanosystems: application to microtubules and the ribosome. *Proc. Natl. Acad. Sci. U. S. A. 98*, 10037−10041.
(25) Tan, Y. S., Reeks, J., Brown, C. J., Thean, D., Ferrer Gago, F. J., Yuen, T. Y., Goh, E. T., Lee, X. E., Jennings, C. E., Joseph, T. L., Lakshminarayanan, R., Lane, D. P., Noble, M. E., and Verma, C. S. (2016) Benzene Probes in Molecular Dynamics Simulations Reveal Novel Binding Sites for Ligand Design. *J. Phys. Chem. Lett. 7*, 3452−3457.
(26) Tan, Y. S., Spring, D. R., Abell, C., and Verma, C. S. (2015) The Application of Ligand-Mapping Molecular Dynamics Simulations to the Rational Design of Peptidic Modulators of Protein-Protein Interactions. *J. Chem. Theory Comput. 11*, 3199−3210.
(27) Satoh, T., Saeki, Y., Hiromoto, T., Wang, Y. H., Uekusa, Y., Yagi, H., Yoshihara, H., Yagi-Utsumi, M., Mizushima, T., Tanaka, K., and Kato, K. (2014) Structural basis for proteasome formation controlled by an assembly chaperone nas2. *Structure 22*, 731−743.
(28) Laskowski, R. A., and Swindells, M. B. (2011) LigPlot+: multiple ligand-protein interaction diagrams for drug discovery. *J. Chem. Inf. Model. 51*, 2778−2786.
(29) Merino-Gracia, J., Costas-Insua, C., Canales, M. A., and Rodriguez-Crespo, I. (2016) Insights into the C-terminal Peptide Binding Specificity of the PDZ Domain of Neuronal Nitric-oxide Synthase: Characterization of the Interaction with the Tight Junction Protein Claudin-3. *J. Biol. Chem. 291*, 11581−11595.
(30) Chi, C. N., Elfstrom, L., Shi, Y., Snall, T., Engstrom, A., and Jemth, P. (2008) Reassessing a sparse energetic network within a single protein domain. *Proc. Natl. Acad. Sci. U. S. A. 105*, 4679−4684.
(31) Morais Cabral, J. H., Petosa, C., Sutcliffe, M. J., Raza, S., Byron, O., Poy, F., Marfatia, S. M., Chishti, A. H., and Liddington, R. C. (1996) Crystal structure of a PDZ domain. *Nature 382*, 649−652.
(32) Petit, C. M., Zhang, J., Sapienza, P. J., Fuentes, E. J., and Lee, A. L. (2009) Hidden dynamic allostery in a PDZ domain. *Proc. Natl. Acad. Sci. U. S. A. 106*, 18249−18254.
(33) Saras, J., and Heldin, C. H. (1996) PDZ domains bind carboxy-terminal sequences of target proteins. *Trends Biochem. Sci. 21*, 455−458.
(34) Dev, K. K. (2004) Making protein interactions druggable: targeting PDZ domains. *Nat. Rev. Drug Discovery 3*, 1047−1056.
(35) Lee, H. J., Wang, N. X., Shi, D. L., and Zheng, J. J. (2009) Sulindac inhibits canonical Wnt signaling by blocking the PDZ domain of the protein Dishevelled. *Angew. Chem., Int. Ed. 48*, 6448−6452.
(36) Hammond, M. C., Harris, B. Z., Lim, W. A., and Bartlett, P. A. (2006) Beta strand peptidomimetics as potent PDZ domain ligands. *Chem. Biol. 13*, 1247−1251.
(37) Hirbec, H., Francis, J. C., Lauri, S. E., Braithwaite, S. P., Coussen, F., Mulle, C., Dev, K. K., Couthino, V., Meyer, G., Isaac, J. T., Collingridge, G. L., and Henley, J. M. (2003) Rapid and differential regulation of AMPA and kainate receptors at hippocampal mossy fibre synapses by PICK1 and GRIP. *Neuron 37*, 625−638.
(38) Daw, M. I., Chittajallu, R., Bortolotto, Z. A., Dev, K. K., Duprat, F., Henley, J. M., Collingridge, G. L., and Isaac, J. T. (2000) PDZ proteins interacting with C-terminal GluR2/3 are involved in a PKC-dependent regulation of AMPA receptors at hippocampal synapses. *Neuron 28*, 873−886.
(39) Songyang, Z., Fanning, A. S., Fu, C., Xu, J., Marfatia, S. M., Chishti, A. H., Crompton, A., Chan, A. C., Anderson, J. M., and Cantley, L. C. (1997) Recognition of unique carboxyl-terminal motifs by distinct PDZ domains. *Science 275*, 73−77.
(40) Doyle, D. A., Lee, A., Lewis, J., Kim, E., Sheng, M., and MacKinnon, R. (1996) Crystal structures of a complexed and peptide-free membrane protein-binding domain: molecular basis of peptide recognition by PDZ. *Cell 85*, 1067−1076.
(41) Nourry, C., Grant, S. G., and Borg, J. P. (2003) PDZ domain proteins: plug and play! *Sci. Signaling 2003*, RE7.
(42) Jemth, P., and Gianni, S. (2007) PDZ domains: folding and binding. *Biochemistry 46*, 8701−8708.
(43) Stiffler, M. A., Chen, J. R., Grantcharova, V. P., Lei, Y., Fuchs, D., Allen, J. E., Zaslavskaia, L. A., and MacBeath, G. (2007) PDZ domain binding selectivity is optimized across the mouse proteome. *Science 317*, 364−369.
(44) Tonikian, R., Zhang, Y., Sazinsky, S. L., Currell, B., Yeh, J. H., Reva, B., Held, H. A., Appleton, B. A., Evangelista, M., Wu, Y., Xin, X., Chan, A. C., Seshagiri, S., Lasky, L. A., Sander, C., Boone, C., Bader, G. D., and Sidhu, S. S. (2008) A specificity map for the PDZ domain family. *PLoS Biol. 6*, No. e239.
(45) Delhommel, F., Chaffotte, A., Terrien, E., Raynal, B., Buc, H., Delepierre, M., Cordier, F., and Wolff, N. (2015) Deciphering the unconventional peptide binding to the PDZ domain of MAST2. *Biochem. J. 469*, 159−168.
(46) Betts, M. J., and Russell, R. B. (2003) Amino Acid Properties and Consequences of Substitutions. In *Bioinformatics for Geneticists* (Barnes, M. R., and Gray, I. C., Eds.) Wiley.
(47) Ernst, A., Appleton, B. A., Ivarsson, Y., Zhang, Y., Gfeller, D., Wiesmann, C., and Sidhu, S. S. (2014) A structural portrait of the PDZ domain family. *J. Mol. Biol. 426*, 3509−3519.

DOI: 10.1021/acs.biochem.9b00308
Biochemistry XXXX, XXX, XXX−XXX